

## EDGE ARTICLE

View Article Online  
View Journal | View IssueCite this: *Chem. Sci.*, 2020, **11**, 3672

All publication charges for this article have been paid for by the Royal Society of Chemistry

## Diazaphosphinanes as hydride, hydrogen atom, proton or electron donors under transition-metal-free conditions: thermodynamics, kinetics, and synthetic applications†

Jingjing Zhang,<sup>a</sup> Jin-Dong Yang <sup>\*a</sup> and Jin-Pei Cheng<sup>\*ab</sup>

Exploration of new hydrogen donors is in large demand in hydrogenation chemistry. Herein, we developed a new 1,3,2-diazaphosphinane **1a**, which can serve as a hydride, hydrogen atom or proton donor without transition-metal mediation. The thermodynamics and kinetics of these three pathways of **1a**, together with those of its analog **1b**, were investigated in acetonitrile. It is noteworthy that, the reduction potentials ( $E_{\text{red}}$ ) of the phosphonium cations **1a**-[P]<sup>+</sup> and **1b**-[P]<sup>+</sup> are extremely low, being  $-1.94$  and  $-2.39$  V (vs.  $\text{Fc}^{+/0}$ ), respectively, enabling corresponding phosphinyl radicals to function as neutral super-electron-donors. Kinetic studies revealed an extraordinarily large kinetic isotope effect KIE(**1a**) of 31.3 for the hydrogen atom transfer from **1a** to the 2,4,6-tri-*(tert-butyl)*-phenoxyl radical, implying a tunneling effect. Furthermore, successful applications of these diverse P–H bond energetic parameters in organic syntheses were exemplified, shedding light on more exploitations of these versatile and powerful diazaphosphinane reagents in organic chemistry.

Received 20th November 2019

Accepted 5th March 2020

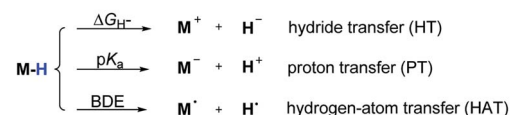
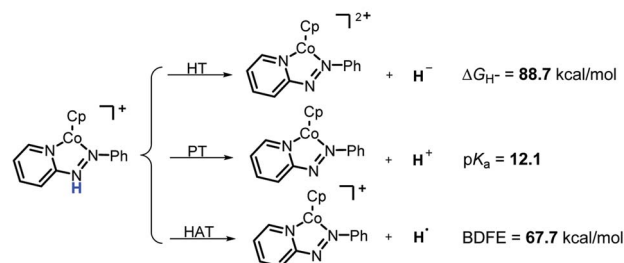
DOI: 10.1039/c9sc05883d

rsc.li/chemical-science

## Introduction

Hydrogen transfer plays a very important role in chemical science and related fields. This process occurs through the cleavage of the targeted R–H bond in three possible pathways (Scheme 1), *i.e.*, hydride ( $\text{H}^-$ ),<sup>1</sup> hydrogen atom ( $\text{H}^\bullet$ )<sup>2</sup> and proton ( $\text{H}^+$ )<sup>3</sup> transfers, which, from a thermodynamic aspect, depends on the R–H bond strength and the nature of the atom bound to the transferred hydrogen atom. Accordingly, knowledge of the relevant thermodynamics of hydricity  $\Delta G_{\text{H}^-}$ ,<sup>1b,c,4</sup> bond-dissociation free-energy, BDFE<sup>5</sup> and acidity,  $\text{p}K_{\text{a}}$ ,<sup>3c,6</sup> as well as the kinetics<sup>7</sup> relevant to these processes would facilitate rational exploitations of new transformations. In recent years, considerable attention has been paid to the development of new hydrogen sources with versatile hydrogen donor reactivities, with particular interests in transition-metal hydrides  $\text{M}-\text{H}$ ,<sup>1c</sup> such as hydrogenase enzyme analogs<sup>8</sup> and hydrogenation catalysts,<sup>9</sup> and main-group organic hydrides  $\text{X}-\text{H}$ ,<sup>1b</sup> such as nicotinamide coenzyme models<sup>10</sup> and Hantzsch esters,<sup>11</sup> and so on.

It is well known that metal hydrides ( $\text{M}-\text{H}$ ) could serve as  $\text{H}^-$ ,  $\text{H}^\bullet$  and  $\text{H}^+$  donors (Scheme 1a).<sup>1c,12</sup> Their diverse hydrogen reactivities originate from the readily modulated polarity of  $\text{M}-\text{H}$  bonds through electronic communication between the

(a) For M–H bonds (*transition-metal system*)(b) For cobalt coordinated N–H bonds (*transition-metal system*)(c) For C–H bonds in triarylmethanes (*transition-metal-free system*)

**Scheme 1** Possible pathways of hydrogen transfers for transition-metal and transition-metal-free systems as well as corresponding thermodynamic driving forces in acetonitrile.

<sup>a</sup>Center of Basic Molecular Science, Department of Chemistry, Tsinghua University, Beijing 100084, China. E-mail: jdyang@mail.tsinghua.edu.cn; jinpei\_cheng@mail.tsinghua.edu.cn

<sup>b</sup>State Key Laboratory of Elemento-Organic Chemistry, College of Chemistry, Nankai University, Tianjin 300071, China

† Electronic supplementary information (ESI) available: Details of syntheses and experimental determinations. CCDC 1947293. For ESI and crystallographic data in CIF or other electronic format see DOI: 10.1039/c9sc05883d

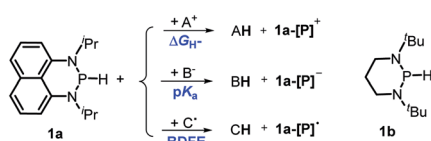


metal centers and coordinated ligands. Compared to an M–H system, the X–H hydride manifested some advantages in mild reaction conditions, good functional-group compatibility, easy modification, *etc.* Integration of these three dissociation possibilities into one X–H covalent bond is a substantial challenge, due to the great disparity in the electronegativity of the X and H fragments. Nevertheless, Waymouth *et al.* very recently reported an excellent new example of such a X–H bond where the N–H bond of the phenylazopyridine ligand in the Co(I) complex can serve as either a  $\text{H}^-$ ,  $\text{H}^+$  or a  $\text{H}^\bullet$  donor (Scheme 1b).<sup>13</sup> It is noted, however, that the diverse reactivity of this N–H bond may require latent electronic communication between the azopyridine ligand and cobalt atom within the five-membered ring, so it may be viewed as a quasi-M–H system.

For a true transition-metal-free system, till now only triaryl-methane analogs, where there exist steric as well as resonance stabilization effects on the incipient radical or charges, were reported to have  $\alpha\text{-C-H}$  bond-cleavage energies determined for all three pathways (Scheme 1c).<sup>14</sup> However, their poor hydrogen donability and severe steric hindrance make these dissociation processes not very useful for synthesis. This, in turn, stimulated our interest to find more useful transition-metal-free X–H systems that promise both the desired energetic measurement and new synthetic applications.

Recently, diazaphospholenium hydrides (P–H) have attracted substantial research interest due to their superior hydricity endowed by the unique diazaphospholene skeleton.<sup>15</sup> Many diazaphospholenes were developed and successfully used in various hydric reductions.<sup>16</sup> However, the superior hydricity resulted in their other promising applications, such as serving as hydrogen atom and proton donors, as well as the precursors of strong electron donors, being greatly overlooked. Considering the similar electronegativity of the hydrogen ( $\chi^{\text{AR}} = 2.20$ ) and phosphorus ( $\chi^{\text{AR}} = 2.06$ ) atoms,<sup>15b</sup> we reckoned that the P–H bond, beside being a good hydride donor,<sup>17</sup> may have the potential to release proton and hydrogen atoms<sup>18</sup> as well, by fine-tuning the electrical properties of the P fragment. And indeed luckily enough, this was realized in the present work.

Herein, we reported a new N-heterocyclic phosphine **1a**, which could act as a  $\text{H}^-$ ,  $\text{H}^+$  and  $\text{H}^\bullet$  donor (Scheme 2). Thermodynamics and kinetics pertinent to these three processes were examined in detail. For comparison, **1b** was investigated as well. Based on the P–H bond energetic studies, we also exploited their versatile applications in the reduction of pyridines, synthesis of bisphosphines, H/D exchange, and activation of carbon–halogen bonds as original examples.



**Scheme 2** P–H reagents **1a** and **1b** serving as diverse hydrogen donors.  $\text{A}^+$ ,  $\text{B}^-$  and  $\text{C}^\bullet$  are the hydride, proton and hydrogen atom acceptors, respectively.

## Results and discussion

### Synthesis

The substrate **1a** was prepared *via* a H/Cl exchange between the corresponding phosphoric chloride and  $\text{LiAlH}_4$  in THF according to the literature<sup>15,17</sup> (see the ESI† for details).  $\text{LiAlD}_4$  was used for deriving the deuterated substrates **1a-D** and **1b-D**. The crystal structure of **1a** was shown in Fig. 1 and features an envelope configuration with the P atom standing out of the naphthalene plane and the P–H bond adopting a flagpole position, similar to the five-membered ring analogs disclosed previously.<sup>15a</sup> And a P–H distance of 1.42(2) Å is slightly shorter than that of the five-membered ring analog.<sup>15</sup>  $^{31}\text{P}$  NMR spectra of **1a** in  $\text{CD}_3\text{CN}$  show a *dt* peak at 25.66 ppm that is split by the hydrogen atoms on the P atom and isopropyl groups. It moves to the higher magnetic field in comparison with other N-heterocyclic phosphines.<sup>17</sup> Under an inert atmosphere, **1a** is stable enough for over 12 hours in tetrahydrofuran, acetonitrile, alcohols, toluene, dimethylsulfoxide and chloroform. On the other hand, **1b** is stable in these solvents as well except in alcohols and chlorinated hydrocarbons, where it decomposes rapidly to yield phosphonites  $(\text{RO})_2\text{PH}^{19}$  or 2-chloro-1,3,2-diazaphosphinane  $[\text{P}]\text{-Cl}$  (Scheme 3), showing that **1b** is more air- and moisture-sensitive than **1a**.

### Redox properties

The oxidation potentials of **1a** and **1b** were examined by cyclic voltammetry (CV), exhibiting a partially reversible oxidation peak of **1a** to  $\text{1a}^{+\bullet}$  at 0.23 V (*vs.*  $\text{Fc}^{+/0}$ , Fig. S1a†) and an irreversible oxidation wave of **1b** at 0.47 V (*vs.*  $\text{Fc}^{+/0}$ , Fig. S1b†) in acetonitrile. The low oxidation potentials of **1a** and **1b** indicate their good reducing capacity. It is interesting to find that **1a** is a better electron donor, in spite of being a far poorer hydride donor than **1b** (*vide infra*). Besides, the redox behaviors of the respective phosphinyl radicals ( $\text{1a}[\text{P}]^\bullet$  and  $\text{1b}[\text{P}]^\bullet$ ) were also

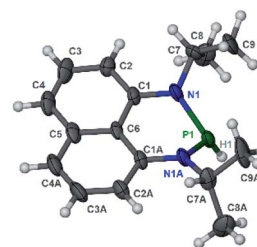
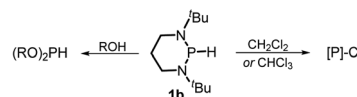


**Fig. 1** The crystal structure of **1a** (50% probability thermal ellipsoids).<sup>20</sup> Selected bond lengths (in Å): P1–H1 1.42(2), P1–N1 1.747(6), N1–C1 1.329(9), N1–C7 1.440(8), and C1–C6 1.413(8).

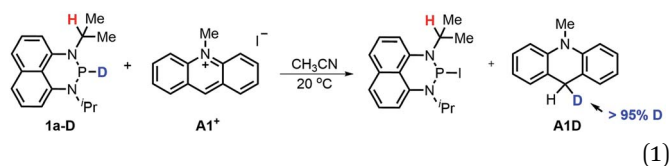


**Scheme 3** Decomposition of **1b** in alcohols and chlorinated hydrocarbons.  $[\text{P}] = (\text{CH}_2)_3(\text{N}^t\text{Bu})_2\text{P}$ , R = Me or Et.

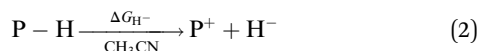
examined through the reduction of the corresponding phosphonium cations (**1a**-[P]<sup>+</sup> and **1b**-[P]<sup>+</sup>), resulting in the CV peaks at −1.94 V and −2.39 V (vs. Fc<sup>+/0</sup>) in acetonitrile, respectively (Fig. S1c and 1d†). The extremely low potentials, especially for **1b**-[P]<sup>+</sup>, indicate the very high reducing capacity of the corresponding **1a**-[P]<sup>•</sup> and **1b**-[P]<sup>•</sup> radicals. This suggests that they both have a very promising potential to serve as a super electron donor in organic synthesis to reduce aryl halides.<sup>22</sup> And indeed, this was verified in the tentative application of the present work in radical hydrodebromination of bromobenzene (see Application part, *vide infra*).

### Thermodynamic driving force and reactivity

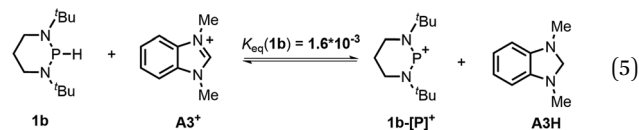
**Hydride transfer (HT).** Hydride transfer from **1a** or **1b**<sup>17</sup> to *N*-methylacridinium iodide **A1**<sup>+</sup> yielded equimolar products (Fig. S3†). To exclude the suspected interruption of the hydridic isopropyl α-C–H, the deuterated substrate **1a-D** was employed, and over 95% deuterated **A1D** was derived (eqn (1) and Fig. S4†). This confirmed that the P–H hydride of **1a** is a stronger donor than that of the isopropyl α-C–H.



The hydricity ( $\Delta G_{\text{H}^-}$ , defined by eqn (2)) of **1a** and **1b** in acetonitrile was determined by measuring their equilibrium constants with the acceptors of known hydricities (eqn (3)). For example, the measured hydride transfer equilibrium constant  $K_{\text{eq}}(\mathbf{1a})$  of 0.48 (equivalent to 0.43 kcal mol<sup>−1</sup>) between **1a** and phenanthridinium trifluoromethanesulfonate **A2**<sup>+</sup> ( $\Delta G_{\text{H}^-}(\mathbf{A2H}) = 61.4$  kcal mol<sup>−1</sup>)<sup>1b</sup> provided the hydricity  $\Delta G_{\text{H}^-}$  of **1a** to be 61.8 kcal mol<sup>−1</sup> (see Fig. S5 in the ESI† for details) and other equilibria (in Fig. S6 and S7†) verified this value, giving a mean hydricity of 62.2 ± 1.0 kcal mol<sup>−1</sup>. This demonstrates **1a** to be a moderate hydride donor, similar to the hydride-donating ability of the NADH analogs.<sup>1b</sup> Thus, it should be capable of reducing commonly used hydride acceptors, such as *N*-methylacridinium cations ( $\Delta G_{\text{H}^-} = 76$  kcal mol<sup>−1</sup>), 9-phenylxanthylum cations (89 kcal mol<sup>−1</sup>) and trityl cations (99 kcal mol<sup>−1</sup>). Similarly, a much lower equilibrium constant  $K_{\text{eq}}(\mathbf{1b})$  of  $1.6 \times 10^{-3}$  (equivalent to 3.8 kcal mol<sup>−1</sup>, eqn (5) and Fig. S8†) established between **1b** and benzimidazolium perchlorate **A3**<sup>+</sup> ( $\Delta G_{\text{H}^-}(\mathbf{A3H}) = 45.0$  kcal mol<sup>−1</sup>)<sup>1b</sup> resulted in  $\Delta G_{\text{H}^-}(\mathbf{1b})$  being 48.8 ± 1.0 kcal mol<sup>−1</sup>, which is comparable to that of the commonly used good hydride donor, 2,3-dihydrobenzo[*d*]imidazoles.<sup>1b</sup> The good hydridic reactivity of **1b** was illustrated in our recent work in the reduction of various unsaturated compounds.<sup>17</sup> It is interesting to note that **1b** is about 13 kcal mol<sup>−1</sup> stronger than **1a** in hydricity, but is 0.24 V weaker in electron-donating ability.



$$\Delta G_{\text{rxn}} = -RT \ln K_{\text{eq}} = \Delta G_{\text{H}^-}(\mathbf{1}) - \Delta G_{\text{H}^-}(\mathbf{AH}) \quad (3)$$



The hydricity can be used to rationalize the disparate reactivity between **1a** and some reported diazaphospholenium hydrides. The latter compounds were reported to react with strong acid HBF<sub>4</sub> to give H<sub>2</sub> and the corresponding phosphonium cations.<sup>15b</sup> However, when **1a** was treated with HBF<sub>4</sub> (or HOTf), no gaseous product was generated. Instead, a new phosphorus species with a doublet peak at about 80 ppm was detected in the <sup>31</sup>P NMR spectrum (Fig. S9a and S9b†). To identify this newly formed species, a base pyridine was added to the reaction mixture, which rendered **1a** the primary product with a small amount of unidentified impurities (Fig. S9c†). Consequently, this mysterious P species was speculated to be protonated **1a** (**1aH**<sup>+</sup>, Scheme 4). Based on the doublet peak of the phosphorus atom in <sup>31</sup>P NMR spectra (if the extraneous proton was connected to the P atom, a triplet <sup>31</sup>P peak would be observed) and the unsymmetrical peaks of naphthyl and isopropyl hydrogen atoms in <sup>1</sup>H NMR spectra (Fig. S10†), the protonated site was thus assigned to the N atom (Scheme 4). We thought that their dissimilarity in reactivity between **1a** and some reported diazaphospholenium hydrides should originate from the relatively weak hydricity of **1a** ( $\Delta G_{\text{H}^-} = 62.2$  kcal mol<sup>−1</sup>). As a consequence, it makes the H<sub>2</sub> release unable to compete with its protonation even under the condition of heating (80 °C for 5 hours). The moderate hydricity of **1a** endows it with good tolerance to even strong acids, avoiding direct elimination of dihydrogen. This in turn offers a possibility for **1a** to act as a hydride donor in acid-catalyzed reduction. Lots of examples in this connection<sup>1a</sup> can be found, especially in the hydrogenation of imines by hydride donors with comparable hydricity to **1a** (~60–70 kcal mol<sup>−1</sup>, like Hantzsch ester,<sup>23</sup> benzothiazoline<sup>24</sup> and cyclohexadiene<sup>25</sup>) under the catalysis of Brønsted acids (for examples BINOL-phosphoric acid, trifluoroacetic acid and Tf<sub>2</sub>NH).

The kinetics of the hydride transfer from **1a** to **A1**<sup>+</sup> was conducted by following the decay of the absorption of **A1**<sup>+</sup> in



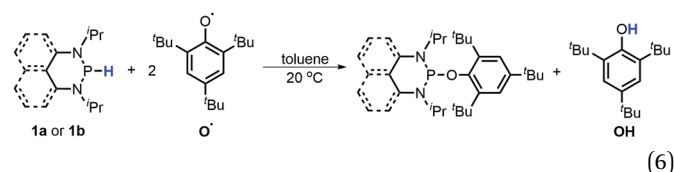
Scheme 4 Protonation of **1a** by HBF<sub>4</sub> and recovery of it by adding pyridine in CD<sub>3</sub>CN.



CH<sub>3</sub>CN at 430 nm with a stopped-flow spectrophotometer (Fig. 2, see the ESI† for details). The second-order rate constant  $k_{\text{HT}}(\mathbf{1a})$  was found to be  $5.94 \text{ M}^{-1} \text{ s}^{-1}$  (Inset in Fig. 2 and Table S1†). Moreover, the nucleophilicity of **1a** can be estimated by the second-order rate constant of the reaction of **1a** with **A1**<sup>+</sup>. Because **1a** has a similar structure with **1b**, based on the nucleophile-specific sensitivity parameter  $s_{\text{N}}$  of **1b** (0.52) and the electrophilicity of **A1**<sup>+</sup> in our recent work,<sup>17</sup> the nucleophilicity  $N$ , of **1a** is estimated to be 8.64. Similarly, the kinetics of **1a-D** with **A1**<sup>+</sup>  $k_{\text{HT}}(\mathbf{1a-D})$  was determined to be  $2.34 \text{ M}^{-1} \text{ s}^{-1}$  (Table S2†). These gave a primary kinetic isotope effect KIE [ $k_{\text{HT}}(\mathbf{1a})/k_{\text{HT}}(\mathbf{1a-D})$ ] of 2.5. A comparison with the previously determined  $k_{\text{HT}}(\mathbf{1b})$  of  $5.41 \times 10^2 \text{ M}^{-1} \text{ s}^{-1}$  for the reaction of **1b** with **A1**<sup>+</sup> in our earlier work<sup>17</sup> indicates that **1b** is about 100 times more reactive than **1a**. This is exactly in accordance with the order of their hydricities ( $\Delta G_{\text{H}}^-$ ) of **1a** vs. **1b** found here.

**Hydrogen atom transfer (HAT).** To examine the possibility of a HAT reaction from diazaphosphinane substrates **1**, the reactions of **1a** and **1b** with the 2,4,6-tri-*tert*-butyl-phenoxy radical **O**<sup>•</sup> were conducted, and yielded 2,4,6-tri-*tert*-butylphenol **OH** and the corresponding phosphorus species (eqn (6)) without generation

of bisphosphines (compared to the reaction of **1a** or **1b** with AIBN, Table 1). A stoichiometric study found a [1]/[O<sup>•</sup>] ratio of 1 : 2, consistent with the product analysis (Fig. S11 and S12†).



To evaluate the hydrogen atom donability of diazaphosphinanes (*i.e.*, P–H BDFE), the thermodynamic cycle was applied on the basis of the  $\Delta G_{\text{H}}^-$  and  $E_{\text{red}}(\text{[P]}^+)$  in hand (Scheme 5 and eqn (7);  $FE_{\text{ox}}(\text{H}^-)$  is  $-26.0 \text{ kcal mol}^{-1}$  in acetonitrile vs.  $\text{Fc}^{0/+}$ ).<sup>26</sup> Substituting the known values into eqn (7)<sup>26a,27</sup> gives P–H BDFEs of  $80.9 \pm 2.0$  and  $77.9 \pm 2.0 \text{ kcal mol}^{-1}$  for **1a** and **1b**, respectively, being comparable with those of phenol and thiophenol antioxidants. Therefore, they could transfer hydrogen atoms smoothly to acceptors with X–H BDFEs around or larger than  $78 \text{ kcal mol}^{-1}$ , such as 2,4,6-tri-*tert*-butylphenoxy **O**<sup>•</sup> ( $77.1 \text{ kcal mol}^{-1}$ ),  $\text{CN}(\text{CH}_3)_2\text{C}^{\bullet}$  (about  $88 \text{ kcal mol}^{-1}$ ) and phenyl radicals ( $104.7 \text{ kcal mol}^{-1}$ ).<sup>5b,28</sup> Compared to **1b**, though the fused aryl groups attenuate the hydricity of **1a** by  $13 \text{ kcal mol}^{-1}$  thermodynamically, they show a negligible effect on the HAT reactivity.

$$\text{BDFE} = \Delta G_{\text{H}}^- - F(E_{\text{red}}(\text{[P]}^+) - E_{\text{ox}}(\text{H}^-)) = \Delta G_{\text{H}}^- - 23.06 E_{\text{red}}(\text{[P]}^+) - 26.0 \text{ (kcal mol}^{-1}) \quad (7)$$

The reaction mechanism of **1a** with radical **O**<sup>•</sup> (eqn (6)) is proposed in Scheme 6 based on the derived thermodynamic data (the reaction of **1b** with **O**<sup>•</sup> is similar). Since hydrogen atom transfer from **1a** to **O**<sup>•</sup> is slightly endothermic ( $\sim 4 \text{ kcal mol}^{-1}$ ), it implies the possibility for a reversible HAT. This reversible HAT



Fig. 2 Monoexponential decay of the absorbance Abs (at 430 nm) with the time  $t$  (s) for the reaction of **1a** ( $3.03 \times 10^{-3} \text{ M}$ ) with **A1**<sup>+</sup> ( $5.00 \times 10^{-5} \text{ M}$ ) in CH<sub>3</sub>CN at 20 °C. Inset: Correlation of  $k_{\text{obs}}$  with  $[\mathbf{1a}]$ .

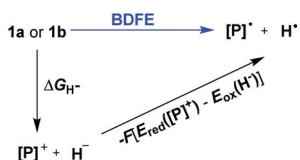
Table 1 Applications of **1a** and **1b** in organic syntheses

Entry	Reactant	Condition	Product	Yield	Type
(1)		<b>1a</b> –[P] <sup>+</sup> (15 mol%), HBpin (1.5 equiv.), CH <sub>3</sub> CN, 80 °C, 36 h		40% <sup>a</sup>	HT
(2)		<sup>t</sup> BuOK, CD <sub>3</sub> CN, 20 °C, 10 min		Quant. <sup>b</sup>	PT
(3)		AIBN (1.5 equiv.), C <sub>6</sub> D <sub>6</sub> , 80 °C, 3 h		>90% <sup>b</sup>	HAT
(4)		<b>1b</b> (1.5 equiv.), AIBN 15 mol%, toluene-d <sub>8</sub> , 90 °C, 5 h		>90% <sup>c</sup>	HAT&ET

<sup>a</sup> Isolated yield. <sup>b</sup> NMR yields determined by the amount of phosphorus species. <sup>c</sup> NMR yields with 1,3,5-trimethoxybenzene as the internal standard.

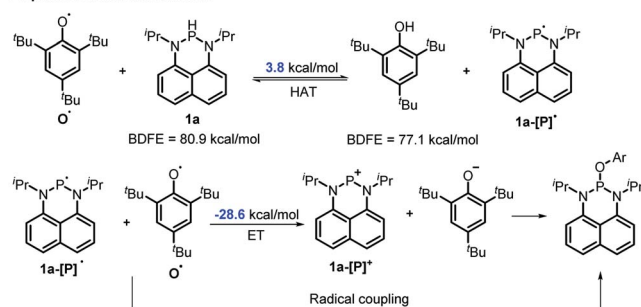






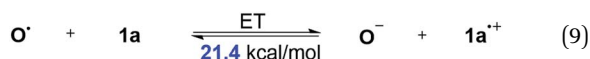
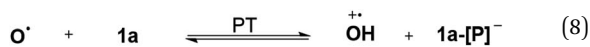
Scheme 5 Thermodynamic cycle for deriving the P-H BDFEs of **1a** and **1b**.

Proposed reaction mechanism:



Scheme 6 The possible mechanism for the reaction of **1a** with  $\text{O}^\bullet$ . Ar = 2,4,6-tri-*tert*-butyl-phenyl group.

could be further driven to the far right by the largely exothermic electron transfer, ET of **1a**–[P] $^\bullet$  radical ( $E_{\text{ox}}(\text{1a}[\text{P}]^\bullet) = -1.94$  V) or a follow-up radical coupling. The observed stoichiometric ratio of 1 : 2 for the reactants [**1**] vs. [ $\text{O}^\bullet$ ] is in exact accordance with the HAT mechanism proposed. On the other hand, a suspected proton transfer between **1a** and the  $\text{O}^\bullet$  radical can be easily ruled out due to the very weak acidity of **1a** (*vide infra*) and strong acidity ( $\text{p}K_{\text{a}}$  of  $\sim -3$ )<sup>5b</sup> reported for the phenol radical cations (eqn (8)). The other suspected possibility, *i.e.* the ET path between **1a** and the  $\text{O}^\bullet$  radical ( $E_{\text{red}} = -0.70$  V<sup>5b</sup>) can also be excluded by a similar strategy on the basis of their respective thermodynamics determined, that indicates that the ET from **1a** to  $\text{O}^\bullet$  is remarkably uphill ( $\Delta G_{\text{ET}} = 21.4$  kcal mol<sup>-1</sup>, eqn (9)).<sup>13,29</sup> It is thus safe to conclude that the initial HAT should be the rate-determining step (RDS) for the reaction expressed in eqn (6).

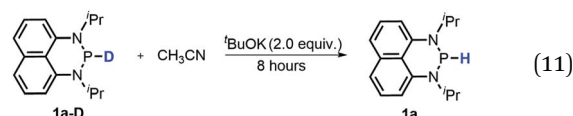
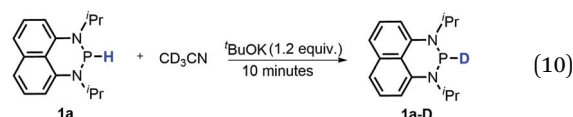


The rate constants of this hydrogen atom transfer from **1a** and **1a-D** to radical  $\text{O}^\bullet$  were measured to be a  $k_{\text{HAT}}(\text{1a})$  of  $0.70 \text{ M}^{-1} \text{ s}^{-1}$  and a  $k_{\text{HAT}}(\text{1a-D})$  of  $2.24 \times 10^{-2} \text{ M}^{-1} \text{ s}^{-1}$ , respectively (Tables S3 and S4<sup>†</sup>). This intermediately points out an extremely large KIE(**1a**) of 31.3, implying a tunneling effect in this HAT process. Such a large KIE has been found in biochemical<sup>30</sup> and transition-metal systems,<sup>31</sup> but seldom observed in organic HAT processes. Similarly, the rate of the analogous HAT of **1b**  $k_{\text{HAT}}(\text{1b})$  was determined to be  $0.74 \text{ M}^{-1} \text{ s}^{-1}$  (Table S5<sup>†</sup>). The quite close  $k_{\text{HAT}}$  for **1a** and **1b** agrees well with their comparable P-H BDFEs (80.9

vs.  $77.9 \text{ kcal mol}^{-1}$ , *vide supra*), verifying their similar HAT reactivity. However, the same kinetic study for **1b-D** gave a  $k_{\text{HAT}}(\text{1b-D})$  of  $0.12 \text{ M}^{-1} \text{ s}^{-1}$  (Table S6<sup>†</sup>), resulting in a primary KIE(**1b**) of 6.2 with no tunneling phenomenon detected.

To understand this discrepancy, temperature-dependent kinetics were further performed (Tables S7–S10<sup>†</sup>). The ratio of Arrhenius pre-factors [ $A(\text{1a})/A(\text{1a-D})$ ] was obtained to be 0.021, and the activation energy difference [ $E_{\text{a}}(\text{1a}) - E_{\text{a}}(\text{1a-D})$ ] was  $-5.53 \text{ kcal mol}^{-1}$  (Fig. S2 and Table S11<sup>†</sup>). These kinetic characteristics [ $A(\text{1a})/A(\text{1a-D}) \ll 1$  and  $E_{\text{a}}(\text{1a}) - E_{\text{a}}(\text{1a-D}) \ll 0$ ] are in fact in line with the tunneling model illustrated by Klinman,<sup>30a</sup> which features a “through-the-barrier” transition state near the top of the classical barrier. In the **1b** system, on the other hand, the normal primary KIE of 6.2,  $A(\text{1b})/A(\text{1b-D})$  of 3.39 and [ $E_{\text{a}}(\text{1b}) - E_{\text{a}}(\text{1b-D})$ ] of  $-0.38 \text{ kcal mol}^{-1}$  all support a classical “over-the-barrier” transition state. A more comprehensive investigation of the tunneling issue is presently underway.

**Proton transfer (PT).** It's known that a good hydride donor usually exhibits poor acidity. This explains why the acidity of widely-used X-H type hydride donors, *e.g.* 2,3-dihydrobenzo[*d*]imidazoles, has never been determined in the absence of metal-coordination. The hydricity of the present N-heterocyclic phosphines is also quite good (*vide supra*), hence an investigation of their acidic reactivity cannot be expected to be too straightforward. Nevertheless, as we learned from the initial failures in deprotonating **1a** or **1b** with some ordinary strong bases, such as 1,8-diazabicyclo[5,4,0]-7-undecene (DBU,  $\text{p}K_{\text{a}} = 24.34$  in  $\text{CH}_3\text{CN}$ ), 1,3,4,6,7,8-hexahydro-2*H*-pyrimido[1,2-*a*]pyrimidine (TBD,  $\text{p}K_{\text{a}} = 26.03$ ) and (*tert*-butylimino)tris(pyrrolidino)-phosphorane (BTPP,  $\text{p}K_{\text{a}} = 28.42$ )<sup>28</sup> (see the ESI<sup>†</sup> for details), we finally found that the H/D exchange of the **1a** P-H proton in the presence of stoichiometric  $^t\text{BuOK}$  in  $\text{CD}_3\text{CN}$  (eqn (10) and Fig. S13<sup>†</sup>) was accomplished in about 10 minutes at room temperature,<sup>32</sup> whereas the same operation for **1a-D** in  $\text{CH}_3\text{CN}$  was finished in 8 hours at room temperature (eqn (11) and Fig. S14<sup>†</sup>). The reversible H/D exchange of **1a** in acetonitrile under the promotion of  $^t\text{BuOK}$  suggested that the acidity of **1a** reaches the measurable acidity limitation in acetonitrile (see the ESI<sup>†</sup> for details).<sup>33</sup> As for **1b** with much stronger hydricity, its acidity is, unfortunately, too weak to examine in solution by any existing experiment. However, it is worth noting that the acidity of a P-H bond can be significantly enhanced upon activation by coordination with transition metals<sup>34</sup> or other Lewis acids.<sup>35</sup>



## Applications in syntheses

Based on the above thermodynamic and kinetic investigations, the potential of applying **1a** and **1b** in organic syntheses, encompassing the diverse hydrogen ( $H^+$ ,  $H^\bullet$  and  $H^-$ ) or electron transfer, was preliminarily explored and showcased herein.

Catalytic reduction of pyridines is a prevailing strategy for the synthesis of dihydropyridines. Recently, Kinjo *et al.*<sup>16g</sup> and Speed *et al.*<sup>36</sup> exploited 1,3,2-diazaphosphenium-catalyzed hydroboration of pyridines with good regio- and chemo-selectivity.<sup>16g</sup> However, in their system, the substrate 3-CN-pyridine gave a mixture of three dihydropyridine isomers. To our delight, we found that under the catalysis of 15 mol% of our **1a**-[P]<sup>+</sup>,<sup>37</sup> the sole 1,4-hydroborated isomer of this reaction was selectively produced in a moderate yield of 40% (entry 1 in Table 1 and Fig. S15†). The good regio-selectivity may be ascribed to the steric factors of the isopropyl group on the nitrogen atom of **1a** based on Kinjo's DFT calculations.<sup>16g</sup> This good regio-selectivity exhibits the catalytic potential of **1a** in the reduction of unsaturated compounds.

Moreover, the acidic character of **1a** (*vide supra*) offers a more economic method for the synthesis of deuterated reagent **1a-D** (entry 2 in Table 1) by employing the much cheaper deuterated solvent  $CD_3CN$  instead of expensive  $LiAlD_4$  in an almost quantitative yield (see the ESI† for details about the synthetic method). Meanwhile, it also provides a new approach for isotope labeling of many other hydridic species. The generation of the hydridic hydrogen from a "protic" solvent as illustrated here may serve as an example of Umpolung which was also proposed by Gudat *et al.* for the P–H bond.<sup>15a</sup>

Since bisphosphines can easily decompose into phosphinyl radicals,<sup>38</sup> they could serve as radical reservoirs for relevant studies and applications. Based on thermodynamic analysis,  $CN(CH_3)_2C^\bullet$  (C–H BDFE  $\approx 85 \text{ kcal mol}^{-1}$ ), generated from the homolysis of azo-bis-isobutyronitrile (AIBN), could abstract the hydrogen atoms from **1a** (P–H BDFE =  $80.9 \text{ kcal mol}^{-1}$ ). Then, the generated phosphinyl radical **1a**-[P]<sup>•</sup> coupled quickly with each other to yield bisphosphines (entry 3 in Table 1, Fig. S16† for **1a** and Fig. S17† for **1b**). The targeted dimers<sup>39</sup> are readily extracted from reaction mixtures in a high yield. This transformation, together with Gudat's photochemical dehydrocoupling,<sup>18</sup> offers easy access to bisphosphines, avoiding complicated and harsh operations and workups required in other synthetic processes using metals such as sodium<sup>38d</sup> and magnesium<sup>38a–c</sup>.

Furthermore, we attempted to design a new radical transformation by an integrated use of hydrogen atoms and electron transfers from N-heterocyclic phosphines. This was inspired by the reactions of AIBN with **1a** and **1b**, where phosphinyl radicals can be easily generated from their P–H precursors through hydrogen atom release. The highly negative oxidation potentials of phosphinyl radicals imply their competency in the reduction of challenging substrates. If a substrate in the reaction system is sufficiently oxidative, its single-electron capture from phosphinyl radicals may be able to compete with radical coupling. In such cases, subsequent transformations may be triggered. Based on the redox potentials of **1b**-[P]<sup>•</sup> ( $E_{ox} = -2.39 \text{ V vs. Fc}^{+/0}$ ,

the same with the  $E_{red}(\mathbf{1b}\text{-[P]}^+)$ ) and bromobenzene ( $E_{red} = -2.8 \text{ V}$ ),<sup>40</sup> hydrodehalogenation of bromobenzene by **1b** was performed in toluene with 15 mol% AIBN as the initiator (entry 4 in Table 1, Fig. S18†). After 5 hours, the expected reduction product, benzene was obtained in over 90% yield. Due to the poor reduction ability of **1a**-[P]<sup>•</sup>, the reaction could not proceed when **1a** was used.<sup>41</sup> Therefore, it could be anticipated that these N-heterocyclic phosphines may open up a promising avenue for the development of super electron donors.

## Conclusions

Hydrogen and electron transfers from phosphines **1a** and **1b** were thermodynamically and kinetically investigated in acetonitrile. The P–H bond of **1a** can participate in reactions involving formal transfer of a hydride/hydrogen atom/proton to a substrate under respective conditions in the absence of the usually required transition-metal- or Lewis acid-mediation. It was observed that **1a** is a moderate hydride and hydrogen atom donor, but a poor Brønsted acid. In comparison, **1b** is a good hydride donor and a moderate hydrogen atom donor; but did not show a detectable acidic reactivity even under the strongest basic solution. With regard to electron donability, **1a** ( $E_{ox}(\mathbf{1a}) = 0.23 \text{ V}$ ) is superior to **1b** ( $E_{ox}(\mathbf{1b}) = 0.47 \text{ V}$ ), contrasting with the order of their hydridic reactivity. Their corresponding phosphinyl radicals are very strong electron donors as reflected by their extremely negative redox potentials. Kinetic studies revealed a tunneling contribution (KIE = 31.3) to the hydrogen atom transfer from **1a** to the phenoxy radical. Based on the derived energetic parameters, their synthetic applications were tentatively exploited. Preliminary results from the synthesis attempts by using the new reagents **1a** and **1b** confirmed their competence as effective hydrogen and electron donors in various redox transformations. The effectiveness of applying the relevant physicochemical parameters in the analysis and design of hydrogen transfer reactions was also shown.

## Conflicts of interest

There are no conflicts to declare.

## Acknowledgements

We are grateful for the financial grants from the National Natural Science Foundation of China (No. 21973052, 21933008, 21602116, and 91745101), the National Science & Technology Fundamental Resource Investigation Program of China (No. 2018FY201200), and the Tsinghua University Initiative Scientific Research Program (No. 20181080083).

## Notes and references

- (a) J.-D. Yang, J. Xue and J.-P. Cheng, *Chem. Soc. Rev.*, 2019, **48**, 2913–2926; (b) S. Ilic, A. Alherz, C. B. Musgrave and K. D. Glusac, *Chem. Soc. Rev.*, 2018, **47**, 2809–2836; (c) E. S. Wiedner, M. B. Chambers, C. L. Pitman,



- R. M. Bullock, A. J. M. Miller and A. M. Appel, *Chem. Rev.*, 2016, **116**, 8655–8692.
- 2 (a) A. Wu and J. M. Mayer, *J. Am. Chem. Soc.*, 2008, **130**, 14745–14754; (b) T. Matsuo and J. M. Mayer, *Inorg. Chem.*, 2005, **44**, 2150–2158; (c) J. M. Mayer, *Acc. Chem. Res.*, 2011, **44**, 36–46.
- 3 (a) Z. Wang, F. Gao, P. Ji and J.-P. Cheng, *Chem. Sci.*, 2018, **9**, 3538–3543; (b) K. Kaupmees, N. Tolstoluzhsky, S. Raja, M. Rueping and I. Leito, *Angew. Chem., Int. Ed.*, 2013, **52**, 11569–11572; (c) J.-D. Yang, P. Ji, X.-S. Xue and J.-P. Cheng, *J. Am. Chem. Soc.*, 2018, **140**, 8611–8623.
- 4 (a) S. Ilic, U. P. Kadel, Y. Basdogan, J. A. Keith and K. D. Glusac, *J. Am. Chem. Soc.*, 2018, **140**, 4569–4579; (b) X.-Q. Zhu, M.-T. Zhang, A. Yu, C.-H. Wang and J.-P. Cheng, *J. Am. Chem. Soc.*, 2008, **130**, 2501–2516.
- 5 (a) M. J. Bezdek and P. J. Chirik, *Angew. Chem., Int. Ed.*, 2018, **57**, 2224–2228; (b) J. J. Warren, T. A. Tronic and J. M. Mayer, *Chem. Rev.*, 2010, **110**, 6961–7001; (c) G. Ali, P. E. VanNatta, D. A. Ramirez, K. M. Light and M. T. Kieber-Emmons, *J. Am. Chem. Soc.*, 2017, **139**, 18448–18451.
- 6 (a) Z. Li, X. Li and J.-P. Cheng, *J. Org. Chem.*, 2017, **82**, 9675–9681; (b) C. Mao, Z. Wang, Z. Wang, P. Ji and J.-P. Cheng, *J. Am. Chem. Soc.*, 2016, **138**, 5523–5526.
- 7 (a) D. Richter and H. Mayr, *Angew. Chem., Int. Ed.*, 2009, **48**, 1958–1961; (b) V. Morozova, P. Mayer and G. Berionni, *Angew. Chem., Int. Ed.*, 2015, **54**, 14508–14512; (c) M. Horn, L. H. Schappele, G. Lang-Wittkowski, H. Mayr and A. R. Ofial, *Chem.–Eur. J.*, 2013, **19**, 249–263; (d) H. Mayr, G. Lang and A. R. Ofial, *J. Am. Chem. Soc.*, 2002, **124**, 4076–4083.
- 8 (a) R. H. Morris, *Chem. Rev.*, 2016, **116**, 8588–8654; (b) M. E. Ahmed, S. Chattopadhyay, L. Wang, D. Brazzolotto, D. Pramanik, D. Aldakov, J. Fize, A. Morozan, M. Gennari, C. Duboc, A. Dey and V. Artero, *Angew. Chem., Int. Ed.*, 2018, **57**, 16001–16004.
- 9 (a) R. Zhong, Z. Wei, W. Zhang, S. Liu and Q. Liu, *Chem.*, 2019, **5**, 1552–1566; (b) W. Ai, R. Zhong, X. Liu and Q. Liu, *Chem. Rev.*, 2019, **119**, 2876–2953.
- 10 (a) Y. Zu, R. J. Shannon and J. Hirst, *J. Am. Chem. Soc.*, 2003, **125**, 6020–6021; (b) A. Bucci, S. Dunn, G. Bellachioma, G. M. Rodriguez, C. Zuccaccia, C. Nervi and A. Macchioni, *ACS Catal.*, 2017, **7**, 7788–7796.
- 11 (a) Q.-A. Chen, M.-W. Chen, C.-B. Yu, L. Shi, D.-S. Wang, Y. Yang and Y.-G. Zhou, *J. Am. Chem. Soc.*, 2011, **133**, 16432–16435; (b) V. N. Wakchaure, P. S. J. Kaib, M. Leutzsch and B. List, *Angew. Chem., Int. Ed.*, 2015, **54**, 11852–11856.
- 12 (a) D. E. Berning, B. C. Noll and D. L. DuBois, *J. Am. Chem. Soc.*, 1999, **121**, 11432–11447; (b) J. R. Norton and J. Sowa, *Chem. Rev.*, 2016, **116**, 8315–8317.
- 13 E. A. McLoughlin, K. M. Waldie, S. Ramakrishnan and R. M. Waymouth, *J. Am. Chem. Soc.*, 2018, **140**, 13233–13241.
- 14 (a) W. S. Matthews, J. E. Bares, J. E. Bartmess, F. G. Bordwell, F. J. Cornforth, G. E. Drucker, Z. Margolin, R. J. McCallum, G. J. McCollum and N. R. Vanier, *J. Am. Chem. Soc.*, 1975, **97**, 7006–7014; (b) X.-M. Zhang, J. W. Bruno and E. Enyinnaya, *J. Org. Chem.*, 1998, **63**, 4671–4678; (c) M. Finn, R. Friedline, N. K. Suleman, C. J. Wohl and J. M. Tanko, *J. Am. Chem. Soc.*, 2004, **126**, 7578–7584; (d) K. Xia, G.-B. Shen and X.-Q. Zhu, *Org. Biomol. Chem.*, 2015, **13**, 6255–6268.
- 15 (a) D. Gudat, A. Haghverdi and M. Nieger, *Angew. Chem., Int. Ed.*, 2000, **39**, 3084–3086; (b) S. Burck, D. Gudat, M. Nieger and W.-W. Du Mont, *J. Am. Chem. Soc.*, 2006, **128**, 3946–3955.
- 16 (a) C. C. Chong, B. Rao and R. Kinjo, *ACS Catal.*, 2017, **7**, 5814–5819; (b) M. R. Adams, C. H. Tien, B. S. N. Huchenski, M. J. Ferguson and A. W. H. Speed, *Angew. Chem., Int. Ed.*, 2017, **56**, 6268–6271; (c) C. C. Chong, H. Hirao and R. Kinjo, *Angew. Chem., Int. Ed.*, 2014, **53**, 3342–3346; (d) C. C. Chong, H. Hirao and R. Kinjo, *Angew. Chem., Int. Ed.*, 2015, **54**, 190–194; (e) C. C. Chong and R. Kinjo, *Angew. Chem., Int. Ed.*, 2015, **54**, 12116–12120; (f) M. R. Adams, C. T. Tien, R. McDonald and A. W. H. Speed, *Angew. Chem., Int. Ed.*, 2017, **56**, 16660–16663; (g) B. Rao, C. C. Chong and R. Kinjo, *J. Am. Chem. Soc.*, 2018, **140**, 652–656; (h) T. Lundrigan, E. N. Welsh, T. Hynes, C.-H. Tien, M. R. Adams, K. R. Roy, K. N. Robertson and A. W. H. Speed, *J. Am. Chem. Soc.*, 2019, **141**, 14083–14088.
- 17 J. Zhang, J.-D. Yang and J.-P. Cheng, *Angew. Chem., Int. Ed.*, 2019, **58**, 5983–5987.
- 18 O. Puntigam, L. Könczöl, L. Nyulászi and D. Gudat, *Angew. Chem., Int. Ed.*, 2015, **54**, 11567–11571.
- 19 R. B. King and P. M. Sundaram, *J. Org. Chem.*, 1984, **49**, 1784–1789.
- 20 A single crystal of **1a** was obtained by volatilization of solution of **1a** in hexane at  $-30\text{ }^{\circ}\text{C}$ . Due to the air- and moisture- sensitivity of this compound, the single crystal could not be fine sealed when X-ray analyzing in the cool air and the minor compound **1a** (about 10%) was oxidized. And in case of the 10% by product, the obtained crystals are of insufficient quality despite several attempts. Thus the quality of the acquired diffraction data was slightly below the average level (see the attached CIF file for details). Despite this, the present X-ray diffraction data confirmed the chemical structure of **1a** unambiguously.
- 21 H. A. Spinney, I. Korobkov, G. A. DiLabio, G. P. A. Yap and D. S. Richeson, *Organometallics*, 2007, **26**, 4972–4982.
- 22 (a) S. S. Hanson, E. Doni, K. T. Traboulsee, G. Coulthard, J. A. Murphy and C. A. Dyker, *Angew. Chem., Int. Ed.*, 2015, **54**, 11236–11239; (b) J. A. Murphy, T. A. Khan, S.-z. Zhou, D. W. Thomson and M. Mahesh, *Angew. Chem., Int. Ed.*, 2005, **44**, 1356–1360; (c) J. A. Murphy, S.-z. Zhou, D. W. Thomson, F. Schoenebeck, M. Mahesh, S. R. Park, T. Tuttle and L. E. A. Berlouis, *Angew. Chem., Int. Ed.*, 2007, **46**, 5178–5183; (d) L. Zhang and L. Jiao, *Chem. Sci.*, 2018, **9**, 2711–2722.
- 23 (a) S. Hoffmann, A. M. Seayad and B. List, *Angew. Chem., Int. Ed.*, 2005, **44**, 7424–7427; (b) R. I. Storer, D. E. Carrera, Y. Ni and D. W. C. MacMillan, *J. Am. Chem. Soc.*, 2006, **128**, 84–86; (c) Q.-A. Chen, K. Gao, Y. Duan, Z.-S. Ye, L. Shi, Y. Yang and Y.-G. Zhou, *J. Am. Chem. Soc.*, 2012, **134**, 2442–2448.
- 24 C. Zhu, K. Saito, M. Yamanaka and T. Akiyama, *Acc. Chem. Res.*, 2015, **48**, 388–398.



- 25 (a) R. P. Thummel, W. E. Cravey and D. B. Cantu, *J. Org. Chem.*, 1980, **45**, 1633–1637; (b) I. Chatterjee and M. Oestreich, *Org. Lett.*, 2016, **18**, 2463–2466.
- 26 (a) V. D. Parker, K. L. Handoo, F. Roness and M. Tilset, *J. Am. Chem. Soc.*, 1991, **113**, 7493–7498; (b) M. Tilset and V. D. Parker, *J. Am. Chem. Soc.*, 1989, **111**, 6711–6717.
- 27 F. G. Bordwell, J.-P. Cheng and J. A. Harrelson, *J. Am. Chem. Soc.*, 1988, **110**, 1229–1231.
- 28 J.-P. Cheng, *et al.*, *Internet Bond-energy Databank (iBonD) Home Page*, <http://ibond.nankai.edu.cn>, accessed at Oct. 2019.
- 29 (a) The energetics of the electron transfer (ET) from **1a** ( $E_{\text{ox}} = 0.23$  V) to the **O**<sup>•</sup> radical ( $E_{\text{red}} = -0.70$  V) shows that its thermodynamic driving force is remarkably uphill ( $\Delta G_{\text{ET}} = 21.4$  kcal mol<sup>-1</sup>), rendering its equilibrium constant close to 0. Such an unfavorable thermodynamic driving force prohibits electron transfer to be a feasible path; (b) J.-P. Cheng, Y. Lu, X.-Q. Zhu and L. Mu, *J. Org. Chem.*, 1998, **63**, 6108–6114.
- 30 (a) J. P. Klinman and A. R. Offenbacher, *Acc. Chem. Res.*, 2018, **51**, 1966–1974; (b) J. C. Price, E. W. Barr, T. E. Glass, C. Krebs and J. M. Bollinger, *J. Am. Chem. Soc.*, 2003, **125**, 13008–13009; (c) J. P. Layfield and S. Hammes-Schiffer, *Chem. Rev.*, 2014, **114**, 3466–3494; (d) M. A. Ehudin, D. A. Quist and K. D. Karlin, *J. Am. Chem. Soc.*, 2019, **141**, 12558–12569.
- 31 (a) E. J. Klinker, S. Shaik, H. Hirao and L. Que Jr, *Angew. Chem., Int. Ed.*, 2009, **48**, 1291–1295; (b) S. H. Bae, X.-X. Li, M. S. Seo, Y.-M. Lee, S. Fukuzumi and W. Nam, *J. Am. Chem. Soc.*, 2019, **141**, 7675–7679.
- 32 When the same reaction was performed in MeOH and toluene solutions (with other conditions identical), none of the H/D exchange was observed.
- 33 A. Kütt, S. Selberg, I. Kaljurand, S. Tshepelevitsh, A. Heering, A. Darnell, K. Kaupmees, M. Piirsalu and I. Leito, *Tetrahedron Lett.*, 2018, **59**, 3738–3748.
- 34 (a) J.-J. Brunet, R. Chauvin, O. Diallo, B. Donnadieu, J. Jaffart and D. Neibecker, *J. Organomet. Chem.*, 1998, **570**, 195–200; (b) P. K. Majhi, A. W. Kyri, A. Schmer, G. Schnakenburg and R. Streubel, *Chem.-Eur. J.*, 2016, **22**, 15413–15419.
- 35 (a) A. Longeau and P. Knochel, *Tetrahedron Lett.*, 1996, **37**, 6099–6102; (b) M. Blum, J. Kappler, S. H. Schindwein, M. Nieger and D. Gudat, *Dalton Trans.*, 2018, **47**, 112–119.
- 36 T. Hynes, E. N. Welsh, R. McDonald, M. J. Ferguson and A. W. H. Speed, *Organometallics*, 2018, **37**, 841–844.
- 37 Although phosphonium triflate **1a**-[P]<sup>+</sup> (as hydride acceptor) is used as a catalyst in the hydride transfer reaction (entry 1 in Table 1), generation of P-H **1a** from **1a**-[P]<sup>+</sup> is the initial step of the catalytic cycle. Then, the pyridine is reduced by *in situ* generated **1a**. The hydride donor **1a** and acceptor **1a**-[P]<sup>+</sup> coexist in the reaction system. Their hydride-donating/accepting abilities (hydricity) are crucial in the catalytic cycle.
- 38 (a) O. Puntigam, D. Förster, N. A. Giffin, S. Burck, J. Bender, F. Ehret, A. D. Hendsbee, M. Nieger, J. D. Masuda and D. Gudat, *Eur. J. Inorg. Chem.*, 2013, **2013**, 2041–2050; (b) R. Edge, R. J. Less, E. J. L. McInnes, K. Müther, V. Naseri, J. M. Rawson and D. S. Wright, *Chem. Commun.*, 2009, 1691–1693; (c) D. Förster, H. Dilger, F. Ehret, M. Nieger and D. Gudat, *Eur. J. Inorg. Chem.*, 2012, **2012**, 3989–3994; (d) N. A. Giffin, A. D. Hendsbee, T. L. Roemmele, M. D. Lumsden, C. C. Pye and J. D. Masuda, *Inorg. Chem.*, 2012, **51**, 11837–11850; (e) J.-P. Bezombes, K. B. Borisenko, P. B. Hitchcock, M. F. Lappert, J. E. Nycz, D. W. H. Rankin and H. E. Robertson, *Dalton Trans.*, 2004, 1980–1988; (f) A. Dumitrescu, V. L. Rudzevich, V. D. Romanenko, A. Mari, W. W. Schoeller, D. Bourissou and G. Bertrand, *Inorg. Chem.*, 2004, **43**, 6546–6548; (g) M. Blum, O. Puntigam, S. Plebst, F. Ehret, J. Bender, M. Nieger and D. Gudat, *Dalton Trans.*, 2016, **45**, 1987–1997.
- 39 E. E. Nifantiev, N. S. Vyazankin, S. F. Sorokina, L. A. Vorobieva, O. A. Vyazankina, D. A. Bravo-Zhivotovskiy and A. R. Bekker, *J. Organomet. Chem.*, 1984, **277**, 211–225.
- 40 (a) C. Costentin, M. Robert and J.-M. Savéant, *J. Am. Chem. Soc.*, 2004, **126**, 16051–16057; (b) L. Pause, M. Robert and J.-M. Savéant, *J. Am. Chem. Soc.*, 1999, **121**, 7158–7159.
- 41 DFT calculations showed that **1a**-[P]<sup>•</sup> and **1b**-[P]<sup>•</sup> should have a comparable ability (with an energy difference of 1.3 kcal mol<sup>-1</sup>, see the ESI† for details) in abstracting the bromine atom. This failed to explain the disparate yields of <10% for **1a**-[P]<sup>•</sup> and 90% for **1b**-[P]<sup>•</sup>. Besides, according to the redox potentials of **1b**-[P]<sup>•</sup> ( $E_{\text{ox}} = -2.39$  V vs. Fc in MeCN) and bromobenzene ( $E_{\text{red}} = -2.8$  V), the electron transfer from **1b**-[P]<sup>•</sup> to bromobenzene is a feasible reversible process, while that for **1a**-[P]<sup>•</sup> ( $E_{\text{ox}} = -1.94$  V) is thermodynamically prohibited. These findings preferentially support an ET-initiated mechanism rather than a direct bromine abstraction.

